

Characteristics, origin, and application potential of Diatomite at Lam Ha ward, Lam Dong province

DINH Quoc Tuan^{1,2*}

¹ Faculty of Geology, University of Science, Ho Chi Minh City, Vietnam

² Vietnam National University, Ho Chi Minh City, Vietnam

* Corresponding email: dqtuan@hcmus.edu.vn

Abstract: *Diatomite in the Lam Ha area, Lam Dong province, primarily belongs to the upper part of the Di Linh Formation (Miocene–Lower Pliocene), where sedimentation was influenced by active tectonics along the Song Ba Fault and intermittent basaltic volcanism. The grain size distribution of diatomite sediments ranges from very fine sand to clay, with a sorting range from poorly sorted to moderately sorted. The skewness of the grain size is predominantly fine-skewed, and the kurtosis varies from platykurtic to highly leptokurtic. The CM pattern, based on the C (1%mm) and M (50%mm) percentiles, indicates sediment deposition in this area is associated with a continental lacustrine or distal floodplain environment with the main channel, characterized by slow-flowing and fluctuating water turbulence. Scanning electron microscopy (SEM) analysis revealed the dominance of *Aulacoseira granulata* species in the diatomite sediments, with particle sizes ranging from 10µm to 30µm. This indicates a similarity in age and paleoenvironmental conditions with the diatomite-bearing sediment in Kostenets, southern Bulgaria. X-ray diffraction (XRD) analysis identified mineral components in the diatomite, including quartz, cristobalite, smectite/montmorillonite, illite and kaolinite, reflecting the combined effects of volcanic input and weathering. Geochemical results show approximately 57.42% SiO₂, 3.96% Fe₂O₃, and various alkali oxides, while the density of diatomite ranges from 1.2 to 2.4 g/cm³. These findings confirm the need for post-depositional processing to meet industrial quality standards. Despite its moderate silica content, targeted acid leaching and thermal treatment can raise SiO₂ purity above 90%, making the processed material suitable for beer filtration and other industrial applications. Beyond economic utility, the abundance of *Aulacoseira granulata* offers insights into Neogene–Pliocene paleoenvironmental conditions. Overall, the Dan Phuong diatomite deposit not only holds promise for local resource development but also contributes to understanding the tectonic and environmental evolution of the region.*

Keywords: *Diatomite, Lam Ha, Lam Dong, Aulacoseira granulata, grain size.*

1. Introduction

Diatomite, a silica-rich sedimentary rock, is formed from the accumulation of diatom frustules, with *Aulacoseira* species often linked to lacustrine or floodplain environments (Yang et al., 2008). Its high porosity, low density, and excellent adsorption capacity make it valuable for industrial uses, including environmental remediation and construction (Tsai et al., 2006). Vietnam holds an estimated 165.5 million tons of diatomite, mainly in the Central Highlands and South-Central regions, with significant deposits in Tuy An (Phu Yen Province) and Lam Dong Province, containing approximately 8 million tons (Phong et al., 2012).

In Lam Dong Province, diatomite is associated with the upper Di Linh Formation. The Lam Ha area, part of this formation, contains Neogene diatoms like *Aulacoseira granulata* and exhibits unique depositional properties. Grain size analysis indicates sediments ranging from very fine sand to clay, deposited in low-energy environments such as lakes or distal floodplains. These conditions, along with SEM analysis, suggest paleoenvironmental similarities to diatomite deposits in Kostenets, Bulgaria (Ognjanova-Rumenova et al., 2018).

This study investigates the sedimentological and mineralogical characteristics of diatomite deposits in Lam Ha, focusing on their characteristics, origin, and application potential. Fieldwork and sedimentological and mineralogical analyses aim to assess their suitability for industrial and environmental applications, contributing to sustainable resource development in Vietnam.

The study area is in Dan Phuong Commune, Lam Ha District, Lam Dong Province, covering approximately 46 km². It is bordered by Da Lat City, Duc Trong District, Di Linh District, and Dak Nong Province, making it a geographically significant location for diatomite research (Fig. 1).

2. Geological background

Lam Ha District, situated on the Di Linh and Lang Biang Plateaus, features an average elevation of over 900 meters. The terrain is complex, dissected by rivers and streams, with three main landforms: steep high mountain slopes in the south and west, undulating low hills in the central areas, and valleys shaped by river erosion, which are ideal for agriculture. The study area in Dan Phuong Commune includes low hills and valleys, characterized by moderate elevation differences (50–100 meters) and basalt-derived soils.

The region's geology is dominated by the Di Linh Formation, dating from the Miocene to Lower Pliocene, composed of lacustrine sediments interbedded with basalt flows. Key components include conglomerate, sandstone, kaolin, bentonite, lignite, and diatomite (DGM, 1999). Diatomite deposits are positioned beneath basalt layers.

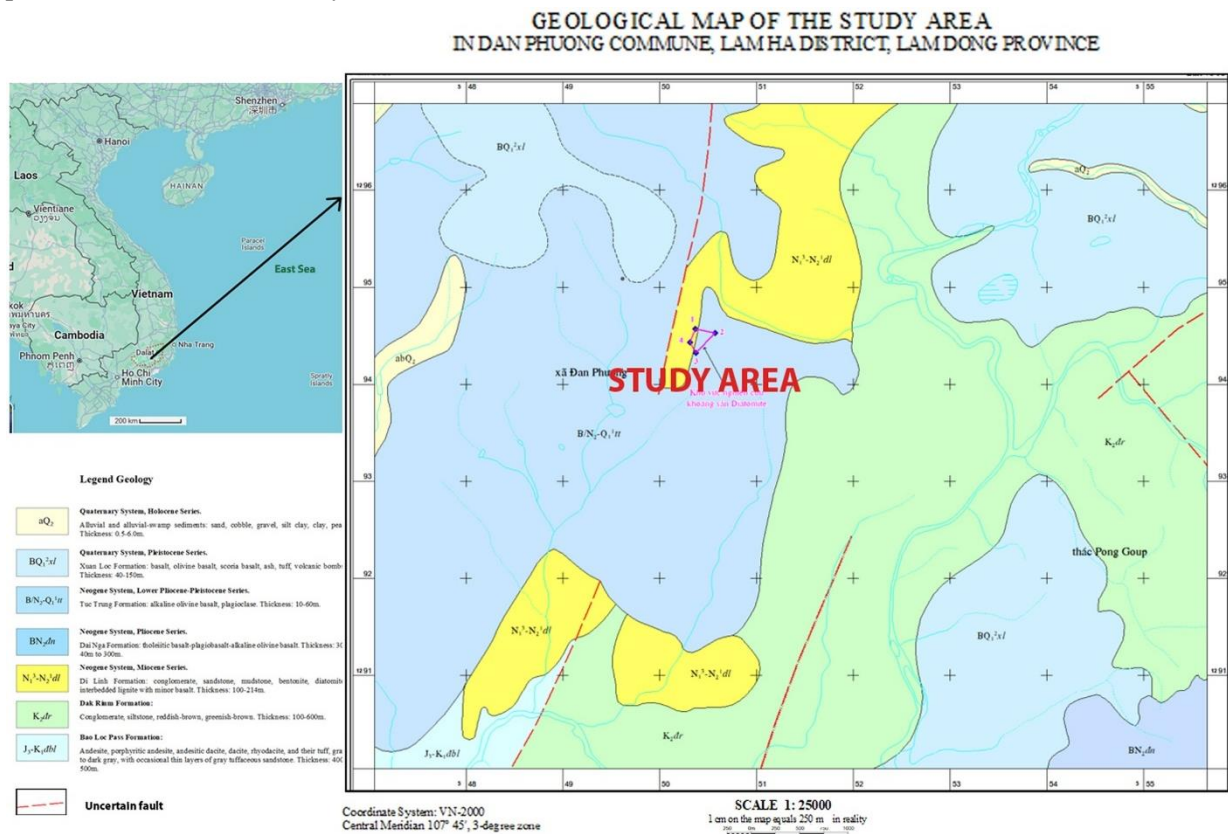


Fig. 1. Schematic geological map of the study area (in Dan Phuong Commune, Lam Ha District, Lam Dong Province) (DGM, 1999)

Additional geological formations include:

- **Bao Loc Pass Formation** (Upper Jurassic - Lower Cretaceous): Andesite, dacite, and tuff.
- **Dak Rium Formation** (Upper Cretaceous): Conglomerate and sandstone from continental sedimentation.
- **Dai Nga Formation** (Pliocene): Basalt flows with lacustrine sediments, rich in construction materials.
- **Tuc Trung Formation** (Pliocene - Lower Pleistocene): Alkaline olivine basalt.
- **Xuan Loc Formation** (Middle Pleistocene): Olivine basalt used in construction.
- **Holocene River Sediments**: Sand, silt, and clay for construction.

Understanding the Di Linh Formation's diatomite and the surrounding geology is essential for assessing the sustainable economic potential of these resources.

3. Methodology

Sample Collection

Eight sediment samples were collected from surface mines in Dan Phuong Commune, Lam Ha District, Lam Dong Province, Vietnam, to analyze grain size distribution and sedimentological characteristics.

Grain Size Analysis

Sieving Method: Fractions >0.063 mm were analyzed to classify fine sand particles.

Hydrometer Analysis: Fractions <0.063 mm were analyzed for silt and clay content.

Grain size parameters, including sorting, skewness, kurtosis, and mean grain size (M_z) (Fig. 2, Fig. 3), were calculated using Folk's (1980) formula. (Table 2a, 2b).

In this study, four statistical parameters proposed by Folk were used to characterize the sediment samples: sorting (σ_I), skewness (Sk_I), kurtosis (K_G), and mean grain size (M_z).

Sorting (σ_I) quantifies how uniform the particle sizes are and is calculated as:

$$\sigma_I = \frac{\phi_{84} - \phi_{16}}{4} + \frac{\phi_{95} - \phi_5}{6.6}.$$

Skewness (Sk_I) describes whether the distribution is dominated by fine or coarse particles, using:

$$Sk_I = \frac{\phi_{16} + \phi_{84} - 2\phi_{50}}{2(\phi_{84} - \phi_{16})} + \frac{\phi_5 + \phi_{95} - 2\phi_{50}}{2(\phi_{95} - \phi_5)}.$$

Kurtosis (K_G) measures the "peakedness" of the distribution—whether it is flatter (platykurtic) or more peaked (leptokurtic)—and is expressed by:

$$K_G = \frac{\phi_{95} - \phi_5}{2.44(\phi_{75} - \phi_{25})}.$$

Lastly, **mean grain size** (M_z) represents the average particle size in the sample and is computed as:

$$M_z = \frac{\phi_{16} + \phi_{50} + \phi_{84}}{3}.$$

Together, these parameters provide a systematic basis for interpreting depositional conditions. Sorting reflects the homogeneity of particle sizes, skewness indicates whether fine or coarse fractions dominate, kurtosis shows the sharpness of the size distribution peak, and mean grain size captures the overall particle-size tendency of the sediment.

CM pattern

The CM pattern method (Passega, 1957; Passega, 1964) was employed to interpret the hydraulic conditions and transport mechanisms responsible for the deposition of diatomite-bearing sediments. Here, C represents the coarsest one-percentile (in microns) on a cumulative grain-size curve, whereas M is the median grain size. Plotting C against M on logarithmic scales creates a CM diagram, whose shape or "pattern" reflects the interplay of processes such as rolling (bedload) and suspension transport. Building upon the foundational C–M approach of Passega (1957, 1964) Bravard and Peiry (1999) conducted extensive field and experimental studies to refine the interpretation of fluvial bedforms. (Fig. 4)

Sample Density Determination

Samples were dried at 110°C for 24 hours, ground, and sieved through a 0.1 mm mesh. Density was measured using a 50 ml pycnometer.

Chemical Composition Analysis

Sample LK 3.1 was analyzed at the Center for Experimental Analysis under the Southern Geological Mapping Federation. Preparation followed TCVN 9924:2013, with methods adhering to TCVN and QTNB standards. Elemental composition was measured using a flame photometer and converted to oxide forms.

X-Ray Diffraction (XRD) Analysis

XRD identified crystalline phases using a PANalytical X'Pert HighScore system with a Cu anode source at 40 kV and 25 mA. The scan range was 5°–89.9° (2θ), providing mineralogical insights. (Fig. 5)

Scanning Electron Microscopy (SEM)

SEM, performed with a JEOL JSM-IT200, revealed microstructural characteristics and diatom morphology using secondary electron detection at 3.0–10.0 kV. The analysis aided in species identification and morphological studies.

4. Results

Physicomechanical properties of diatomite

The diatomaceous clay is light gray, sometimes with a yellowish tint, porous, and has a laminated structure. Its density ranges from 1.29 to 2.39 g/cm³, and its moisture content varies from 4.70% to 31.72%.

Sedimentological characteristics

Diatomaceous earth is found in the uppermost layer of the Di Linh Formation, with a thickness of about 60 meters, occasionally interbedded with basalt.

Data Analysis of Grain Size Parameters

The sedimentological analysis of samples from the study area reveals diverse depositional conditions based on sorting, skewness, kurtosis, and mean grain size. Sorting values range from "Very Poorly Sorted" (2.04–2.70) in samples LK-1.1, LK-3.1, LK-3.2, and LK II, indicating a broad particle size range and fluctuating energy conditions, to "Moderately Sorted" (0.97) in sample LK-2.1, reflecting more uniform deposition in stable settings. Skewness analysis highlights a dominance of finer particles in most samples, classified as "Strongly Fine-Skewed" (0.74–0.85), typical of low-energy environments, while sample LK I, with "Strongly Coarse-Skewed" (-0.57) characteristics, suggests high-energy conditions. Kurtosis values indicate varied distribution patterns, with "Very Platykurtic" samples (0.43–0.49) such as LK-1.1, LK-3.1, and LK-3.2 reflecting flat, stable deposition, and "Extremely Leptokurtic" samples (1.22–5.13), such as LK-2.1 and LK II, showing sharp, peaked distributions associated with low-energy environments. Mean grain size (Mz) analysis further supports these observations, with sample LK I exhibiting fine silt (6.89 phi), indicative of low-energy conditions, sample LK II containing very fine sand (3.83 phi) associated with moderate energy, and other samples showing intermediate grain sizes (4.00–5.40 phi), consistent with deposition in low-to-moderate energy lacustrine or floodplain settings (Fig. 4). These results reflect the complexity of the depositional environment and the influence of energy variations on sediment characteristics.

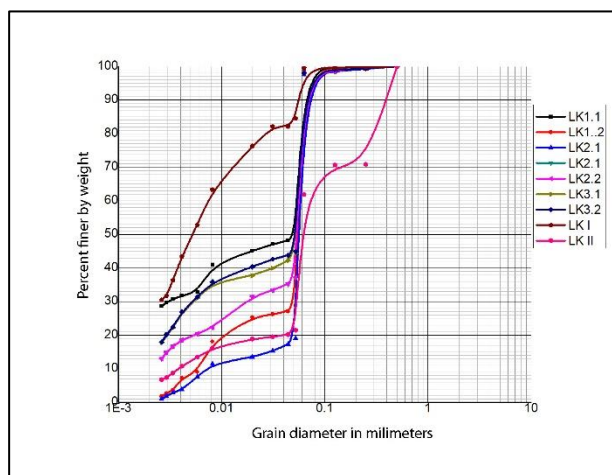


Fig. 2. Cumulative curves of the grain-size distribution

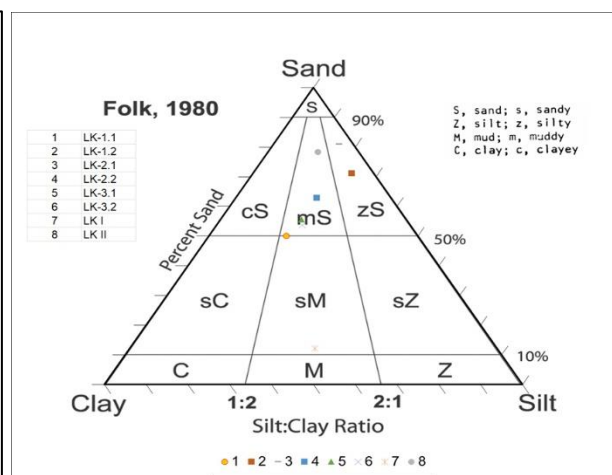


Fig. 3. Triangle diagram: Sand-Silt-Clay

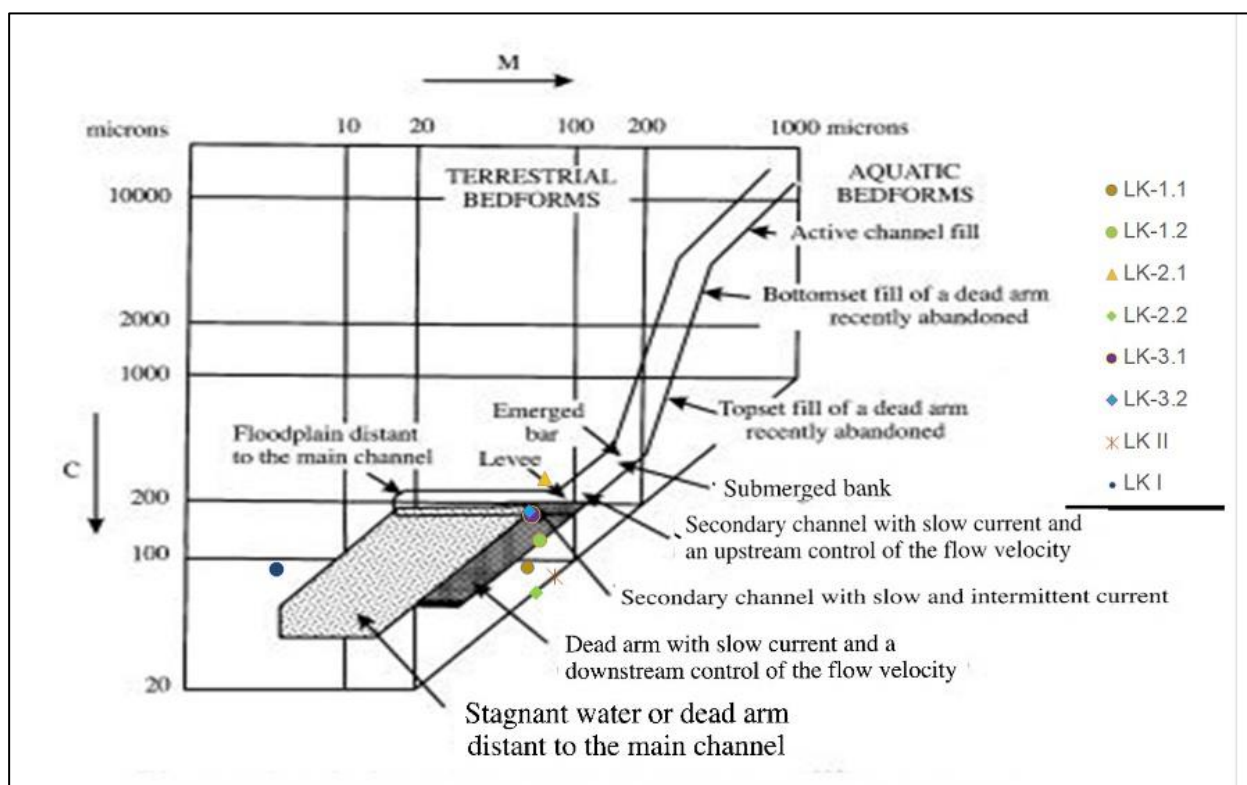


Fig. 4. CM Pattern and Associated Bedforms (after Peiry 1988) with 8 samples in study area

Chemical analysis of the diatomite

The chemical compositions of natural diatomite from Lam Ha and Dai Lao (Phong et al, 2012) (for comparison) are presented in Table 1.

Tab. 1. The chemical compositions of natural diatomite from Lam Ha and Dai Lao [% wt.]

	SiO ₂	Al ₂ O ₃	Fe ₂ O ₃	FeO	CaO	MgO	Na ₂ O	K ₂ O	TiO ₂	MnO	P ₂ O ₅	L.O.I	SO ₃	H ₂ O
Lam Ha-Lam Dong	57.42	21.67	3.96	0.32	0.60	1.23	0.35	1.41	0.69	0.02	0.35	10.77	<0.01	8.25
Dai Lao - Lam Dong	52.90	22.90	5.32	-	0.43	0.26	0.51	1.25	0.15	-	-	19.80	-	-

The chemical composition of diatomite from Lam Ha (Lam Dong) shows a relatively high SiO₂ content (approximately 57.42% wt), accompanied by a significant amount of Al₂O₃ (21.67% wt) and certain proportions of Fe₂O₃ (3.96% wt) and FeO (0.32% wt). Alkali and alkaline earth oxides such as CaO (0.60% wt), MgO (1.23% wt), Na₂O (0.35% wt), and K₂O (1.41% wt) are also present in moderate proportions. Additionally, the sample contains TiO₂ (0.69% wt), MnO (0.02% wt), and P₂O₅ (0.35% wt), with a loss on ignition (L.O.I) of 10.77% wt, very low SO₃ content (<0.01% wt), and an H₂O content of 8.25% wt.

Compared to the diatomite sample from Dai Lao (Lam Dong), the Lam Ha diatomite exhibits a higher SiO₂ content and lower Fe₂O₃ content, but elevated levels of MgO, TiO₂, and P₂O₅. These differences indicate variations in the geochemical composition that reflect distinct formation conditions or sedimentary origins. Despite these variations, similarities in their overall composition suggest comparable depositional environments and processes in both areas.

to distinguish cristobalite from quartz and tridymite, the scan range was extended, enabling confirmation through a secondary diagnostic peak at approximately 36.1° (2θ).

Scanning Electron Microscopy (SEM)

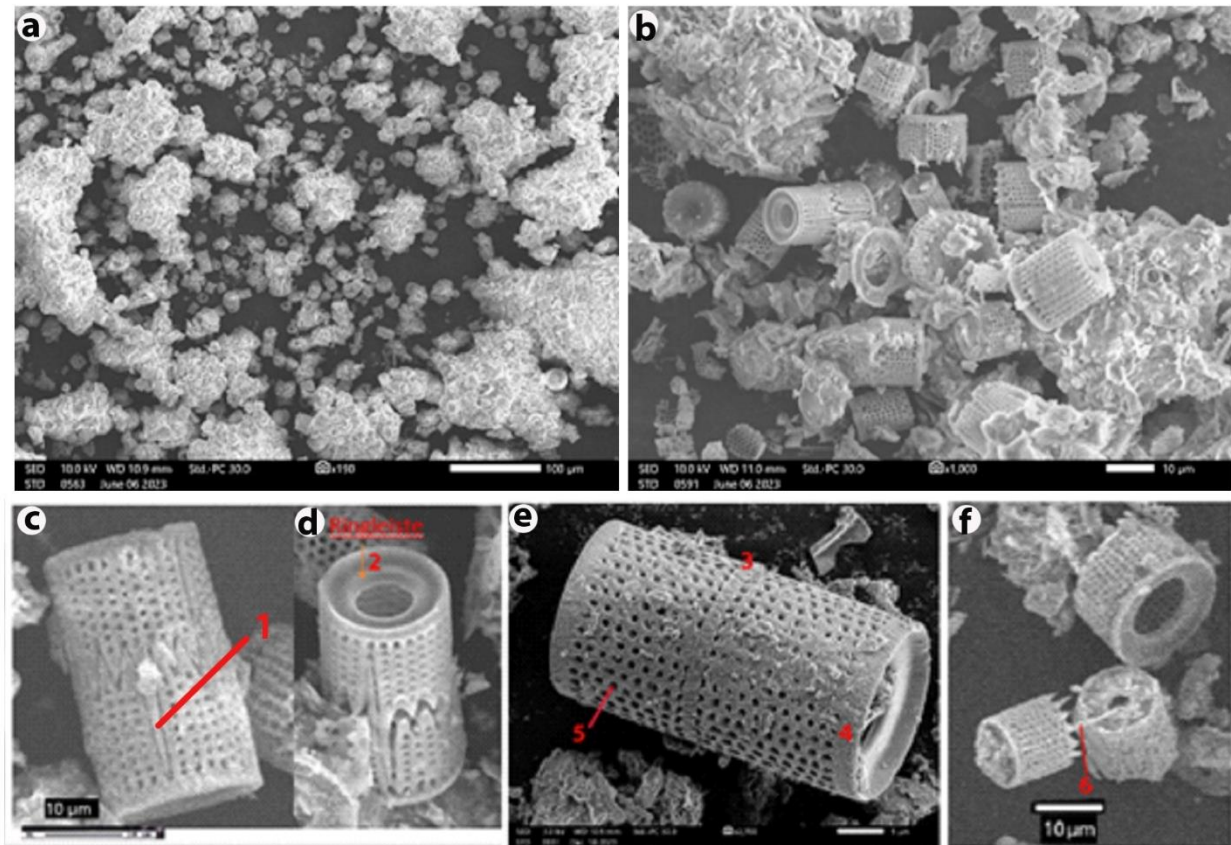


Fig. 6. Scanning electron micrographs of raw diatomite from Dan Phuong – Lam Ha – Lam Dong, showing the diatom species *Aulacoseira granulata*; a- Diatomite observed under SEM at 110× magnification, displaying an overview of diatom distribution and matrix, b- SEM image at 1000× magnification, showing detailed diatom frustule structures, c, d, e, f- Frustule fragments of *Aulacoseira granulata* with key morphological characteristics: 1 – Cylindrical shape with separation valves bearing both short and long spines; 2 – Ringleiste may be present; 3 – Frustules forming colonies joined by spines; 4 – Collum may be present; 5 – Square-shaped mantle areolae; 6 – Separation valves often possessing very long spines.

The natural diatomite sample was finely ground using a 0.1 mm sieve and subsequently analyzed using a scanning electron microscope (SEM) (Fig. 6). The observed morphology of the diatoms exhibited a cylindrical shape, with frustule fragment sizes ranging from 10 to 30 μm . The diatoms identified in the sediment sample were characterized based on six key morphological features: (1) Cylindrical shape with separation valves bearing both short and long spines; (2) Presence of a ringleiste; (3) Frustules forming colonies connected by spines; (4) Possible presence of a collum; (5) Square-shaped areolae on the mantle; and (6) Separation valves often featuring one or two very long spines.

These distinguishing features were documented using scanning electron microscopy (SEM), as outlined by Krammer and Lange-Bertalot (1986–1991) and Hasle and Syvertsen (1996), enabling the identification of the diatom species *Aulacoseira granulata*.

Aulacoseira granulata is a centric diatom species (belonging to the Bacillariophyceae group), commonly found in freshwater ecosystems. This species is frequently used as a biological indicator in water quality studies and paleoecology research (Round, Crawford, & Mann, 1990).

Tab. 2a. Grain-size classes and statistical parameters of grain-size distribution Folk (1980)

N	SAM	SORTIN		SKEW		KURT		MEAN
o	PLE	G (phi)	σ_I	NESS	Sk_I	OSIS	K_G	GRAIN SIZE
								(phi)

1	LK-1.1	2.05	Very Poorly Sorted	0.82	Strongly Fine-Skewed	0.44	Very Platykurtic	5.40
2	LK-1.2	1.57	Poorly Sorted	0.84	Strongly Fine-Skewed	0.91	Mesokurtic	4.78
3	LK-2.1	0.97	Moderately Sorted	0.74	Strongly Fine-Skewed	5.13	Extremely Leptokurtic	4.00
4	LK-2.2	1.97	Poorly Sorted	0.85	Strongly Fine-Skewed	0.73	Platykurtic	5.23
5	LK-3.1	2.04	Very Poorly Sorted	0.84	Strongly Fine-Skewed	0.49	Very Platykurtic	5.35
6	LK-3.2	2.05	Very Poorly Sorted	0.82	Strongly Fine-Skewed	0.49	Very Platykurtic	5.38
7	LK I	1.85	Poorly Sorted	-0.58	Strongly Coarse-Skewed	0.78	Platykurtic	6.89
8	LK II	2.70	Very Poorly Sorted	0.19	Fine-Skewed	1.23	Leptokurtic	3.83

Tab. 2b. Grain-size classes and physical properties

No	SAMPLE	Mz	% Sand	% Silt	% Clay	1%mm (C)	50%mm (M)	DENSITY (g/cm ³)	MOISTURE (%)
1	LK-1.1	Medium silt	50.01	18.54	31.45	93.75	62.67	2.36	18.84
2	LK-1.2	Coarse silt	71.15	23.58	5.27	131.40	71.65	2.39	4.78
3	LK-2.1	Coarse silt	81.04	15.61	3.35	290.38	75.00	2.37	13.73
4	LK-2.2	Medium silt	62.92	19.25	17.84	245.54	68.68	1.29	8.38
5	LK-3.1	Medium silt	55.63	19.37	25.00	181.62	65.79	2.04	30.09
6	LK-3.2	Medium silt	53.70	20.46	25.84	191.18	64.26	2.20	31.72
7	LK I	Fine silt	12.12	44.29	43.59	92.27	4.85	2.07	14.31
8	LK II	Very fine sand	78.37	11.85	9.78	732.55	83.50	2.50	12.59

5. Discussion

The geological and sedimentological characteristics of the Dan Phuong diatomite deposit in Lam Ha, Lam Dong province, provide significant insights into the paleoenvironmental conditions and tectonic history of the region. The vigorous tectonic activity of the Song Ba Fault from the Late Miocene to the Quaternary (N₁³-Q) played a crucial role in shaping the depositional environment. The formation of grabens

along the Song Ba River facilitated the accumulation of terrigenous sediments, including diatomite Di Linh Formation (Bach et al., 2013). This tectonic framework not only influenced sediment supply and accommodation space but also affected the hydrodynamic conditions within the basin.

Stratigraphically, the Di Linh Formation in the upper section is predominantly composed of diatomite, primarily consisting of *Aulacoseira granulata*. This formation, dating from the Miocene to the Lower Pliocene, is characterized by lacustrine sediments interbedded with basalt flows (Fig. 7), indicating a dynamic interplay between sedimentation and volcanic activity. The presence of basalt flows suggests periodic volcanic eruptions, which may have contributed to the sedimentary processes through the input of volcanic ash and the alteration of hydrological regimes.



Fig. 7. Stratigraphic Relationship Between Diatomite and Basalt flows (weathered basalt) The diatomite is overlain by a layer of basalt (weathered basalt), with the boundary marked by a red dashed line.

Sedimentological analysis of eight samples from the Dan Phuong–Lam Ha–Lam Dong area reveals a predominance of silt to very fine sand sediments. The sedimentary architecture parameters indicate deposition in low-energy environments such as lakes, floodplains, or secondary flow channels. The poor to medium sorting and slight flow fluctuations, as evidenced by the CM diagrams (Fig 4), suggest that these sediments were deposited under conditions of variable energy, likely influenced by seasonal hydrological changes and tectonic-induced landscape modifications.

Mineralogically, the diatomite samples exhibit a composition of approximately 57.42% wt. SiO_2 and 3.96% wt. Fe_2O_3 , alongside the presence of alkali oxides. The mineral assemblage includes quartz and illite from detrital inputs, kaolinite and smectite as weathering products, and cristobalite indicative of possible volcanic influence. This diverse mineralogy points to a complex depositional environment influenced by both climatic factors and tectonic processes. The relatively high silica content, although below the ideal threshold for certain industrial applications, combined with the presence of impurities such as Al_2O_3 and Fe_2O_3 , underscores the necessity for post-depositional processing to enhance the quality of the diatomite for specific uses (Phong et al., 2012).

Biologically, *Aulacoseira granulata* is the predominant diatom species identified in the analyzed samples. The presence of *Aulacoseira granulata* in the depositional environment is indicative of eutrophic conditions, as *Aulacoseira granulata* thrives in nutrient-rich, slightly alkaline waters with moderate conductivity. The presence of this species serves as a valuable paleoenvironmental indicator, reflecting past nutrient dynamics and water quality. Furthermore, the association of *Aulacoseira granulata* with specific sedimentological and mineralogical features enhances our understanding of the interplay between biological productivity and environmental conditions during the Neogene to Pliocene epochs.

Significance of *Aulacoseira granulata* in Reconstructing Paleoenvironmental Conditions.

Aulacoseira granulata is a key species in temperate, subtropical, and tropical eutrophic reservoirs (Reynolds et al., 2002; Borges et al., 2008; Vyverman, 1996). It frequently dominates phytoplankton communities, particularly in river-floodplain systems (Yang et al., 2008), and exhibits the ability to utilize organic iron complexes (Naito et al., 2006). This species is often found in regions near volcanic activity,

where eruptions can influence lacustrine sediment quality, posing challenges for reconstructing past environmental changes.

The response of *Aulacoseira granulata* to tephra deposition highlights its ecological sensitivity. Initially, tephra input causes a decline in *Aulacoseira granulata* abundance due to nutrient limitations. The dissolution of tephra releases silica into the water, but buried phosphorus in sediments limits nutrient availability. As *Aulacoseira granulata* is a poor competitor under nutrient-deficient conditions, it is displaced by other taxa (Barker et al., 2000; Barker et al., 2003; Kilham et al., 1986). Once nutrient levels stabilize, *Aulacoseira granulata* abundance recovers to pre-disturbance levels, reflecting its resilience in nutrient-enriched environments.

According to Bere et al. (2009), *Aulacoseira granulata* thrives in water with gradients of conductivity ranging from 25.96 to 324.76 $\mu\text{S}\cdot\text{cm}^{-1}$, pH between 6.61 and 7.54, with slightly alkaline upstream waters being favorable its presence. This finding aligns with sedimentological and mineralogical studies of the Dan Phuong diatomite, highlighting its significance as a paleoenvironmental archive. The diatomite in this region provides valuable information for reconstructing ancient depositional environments, including nutrient dynamics and the impacts of volcanic activity on aquatic ecosystems (Suhry et al., 2020b). The sensitivity of *Aulacoseira granulata* to nutrient fluxes and competitive interactions further emphasizes its importance in understanding historical ecological changes.

Potential Applications and Sustainable Development Directions for Diatomite from Dan Phuong, Lam Ha, Lam Dong

The production of filter aids utilizing diatomite sourced from the Dan Phuong deposit in Lam Ha, Lam Dong province, has been investigated. Initial findings reveal that raw diatomite contains an average SiO_2 content of approximately 57.42%, which is below the ideal threshold for filter aids, alongside higher levels of impurities such as Al_2O_3 and Fe_2O_3 . These impurities can negatively affect the quality of beer filtration.

A study by Phong and Dang, titled *Preparation of Filter Aids Based on Lam Dong Diatomite*, employed an acid leaching method using 6M H_2SO_4 at 90–95°C to enrich SiO_2 content and reduce impurities. The material was subsequently calcined at high temperatures (900–1250°C) to enhance its properties. The best results were achieved after 24–36 hours of acid leaching and calcination at 900°C, producing a filter aid with significantly increased SiO_2 content (above 90%) and reduced impurities (Phong et al., 2012).

Thus, after appropriate processing, diatomite from Dan Phuong, Lam Ha, Lam Dong, can be utilized to produce filter aids that meet beer filtration standards. However, due to its high impurity content and relatively low raw SiO_2 concentration, untreated diatomite is unsuitable for this application and requires extensive processing to improve its quality. This highlights the potential of Lam Dong diatomite as a domestic source of filter aids, reducing reliance on imported products.

6. Conclusion

The diatomite deposit at Dan Phuong, Lam Ha District, Lam Dong Province, presents a multifaceted record of tectonically influenced sedimentation, volcanic input, and biological productivity from the Miocene to Lower Pliocene. Detailed grain-size analyses reveal that the diatomite is dominantly fine-grained (silt to very fine sand), formed under low-to-moderate energy conditions in lacustrine or distal floodplain settings, as corroborated by the CM pattern results. Mineralogical and SEM examinations underscore the significant contribution of volcanic components (e.g., cristobalite) and detrital minerals (e.g., illite, smectite/ montmorillonite), while the diatom assemblage—marked by the prevalence of *Aulacoseira granulata*—attests to nutrient-rich, slightly alkaline paleoenvironments. These findings collectively illustrate the intricate interplay between tectonics along the Song Ba Fault, episodic volcanism, and biological productivity in shaping diatomite formation.

From an applied perspective, the moderate silica content (~57.42%) underscores the need for post-depositional processing (acid leaching and calcination) to meet industrial-grade specifications for filter aids, notably in beer filtration and environmental remediation. Although raw diatomite falls below ideal standards, successful enrichment of SiO_2 to above 90% highlights its potential to reduce reliance on imported filter materials. Nonetheless, future research should address the economic feasibility of large-scale processing and evaluate the environmental impacts of diatomite extraction.

Methodologically, this work emphasizes the value of integrated sedimentological, mineralogical, and biological analyses to reconstruct paleoenvironmental conditions. The dominance of *Aulacoseira granulata* provides an instructive case for using diatoms as paleoenvironmental proxies, capturing fluctuations in nutrient supply and volcanic influences. However, broader stratigraphic correlations and additional geochemical tracers would refine our understanding of diatomite quality variability and resource extent.

Overall, this study advances the geological framework for diatomite deposits in Lam Ha, clarifies their genesis in a volcanically and tectonically dynamic basin, and outlines the industrial potential of these resources. Future efforts should include detailed cost-benefit assessments of beneficiation processes, closer scrutiny of impurity distributions, and expanded field surveys to ascertain resource longevity. By addressing these objectives, the diatomite deposits can be leveraged both scientifically—for refining Neogene–Pliocene paleogeographic models—and economically—to foster sustainable development of local mineral resources.

Tables and figures (with descriptions)

Tables:

Table 1 - Chemical Compositions of Natural Diatomite from Lam Ha and Dai Lao [% wt.]

Provides a comparative analysis of chemical compositions, highlighting major elements like SiO₂, Al₂O₃, Fe₂O₃, and others.

Shows the higher SiO₂ content in Lam Ha diatomite and variations in elements like MgO, TiO₂, and Fe₂O₃, reflecting differences in formation conditions.

Table 2a - Grain-size Classes and Statistical Parameters (Folk and Ward, 1957)

Details sorting, skewness, kurtosis, and mean grain size for each sample.

Indicates depositional environments, with sorting values ranging from "Very Poorly Sorted" to "Moderately Sorted."

Table 2b - Grain-size Distribution and Physical Properties

Describes sand, silt, and clay percentages, density, and moisture content.

Reflects the variability in depositional energy and sediment characteristics.

Figures:

Figure 1 - Schematic Geological Map of the Study Area

Displays the geological formations within Dan Phuong Commune, Lam Ha District.

Highlights the spatial distribution of formations like the Di Linh Formation and associated diatomite deposits.

Figure 2 - Cumulative Curves of Grain-size Distribution

Visualizes the particle size distribution for sediment samples, aiding in the interpretation of depositional processes.

Figure 3 - Triangle Diagram: Sand-Silt-Clay

Represents the proportions of sand, silt, and clay in the samples, categorizing sediments by textural classes.

Figure 4 - CM Pattern and Associated Bedforms (After Peiry, 1988)

Provides insights into depositional environments by linking grain size and flow energy.

Reflects the dynamic nature of sediment transport in lacustrine and floodplain settings.

Figure 5 - The XRD pattern of raw Dan Phuong, Lam Ha, Lam Dong diatomite; a- XRD analysis of four samples (LK-1.1 (black), LK-I (orange), LK-2.1 (blue), LK-3.1 (pink)) with a scan range of 5°–30° (2θ), showing the presence of smectite, kaolinite, illite, and quartz. b- XRD analysis of sample LK-3.1 (red) show with an extended scan range of 5°–89.9° (2θ), allowing identification of kaolinite, montmorillonite, quartz, and cristobalite. The main diagnostic peak of cristobalite is observed at approximately 21.8° (2θ). However, to distinguish cristobalite from quartz and tridymite, the scan range was extended, enabling confirmation through a secondary diagnostic peak at approximately 36.1° (2θ).

Highlights the mineralogical composition of diatomite samples, identifying key phases such as quartz, cristobalite, and clays.

Demonstrates the mineral variability between samples.

Figure 6 - Scanning electron micrographs of raw diatomite from Dan Phuong – Lam Ha – Lam Dong, showing the diatom species *Aulacoseira granulata*; a- Diatomite observed under SEM at 110× magnification, displaying an overview of diatom distribution and matrix, b- SEM image at 1000× magnification, showing detailed diatom frustule structures, c, d, e, f- Frustule fragments of *Aulacoseira granulata* with key morphological characteristics: 1 – Cylindrical shape with separation valves bearing both short and long spines; 2 – Ringleiste may be present; 3 – Frustules forming colonies joined by spines; 4 – Collum may be present; 5 – Square-shaped mantle areolae; 6 – Separation valves often possessing very long spines.

Showcases the morphological features of diatoms, including *Aulacoseira granulata*, under SEM.

Highlights the structural characteristics like cylindrical frustules, ringleiste, and spines.

Figure 7 - Stratigraphic Relationship Between Diatomite and Basalt flows (weathered basalt)

The diatomite is overlain by a layer of basalt (weathered basalt), with the boundary marked by a red dashed line. The image shows the diatomite layer, part of the upper Di Linh Formation, overlain by weathered basalt. This contact reflects volcanic activity influencing sedimentation during the Miocene to Lower Pliocene.

Acknowledgements

This research is funded by University of Science, VNU-HCM under grant number T2023-51. Authors thank the anonymous reviewers for improving the paper.

Literature - References

1. Bach, H. V., Du Hung, N., Cảnh, Đ. V., Tâm, N. M., & Hoài, T. T. T. (2013). Eastern sea spreading and the development of Phu Khanh basin: updated from the results of new 2D seismic interpretation. *Vietnam Journal of Earth Sciences*, 35(3), 249–257.
2. Barker, P., Telford, R., Merdaci, Q., Williamson, D., Taieb, M., Vincens, A., et al. (2000). The sensitivity of a Tanzanian crater lake to catastrophic tephra input and four millennia of climate change. *Holocene*, 10, 303–310.
3. Barker, P., Williamson, D., Gasse, F., & Gilbert, E. (2003). Climatic and volcanic forcing revealed in a 50,000-year diatom record from Lake Massoko, Tanzania. *Quaternary Research*, 60, 368–376.
4. Bere, T., & Tundisi, J. G. (2009). Weighted average regression and calibration of conductivity and pH of benthic diatom assemblages in streams influenced by urban pollution–São Carlos/SP, Brazil. *Acta Limnol. Bras*, 21(3), 317–325.
5. Biscaye, P. E. (1965). Mineralogy and sedimentation of recent deep-sea clay in the Atlantic Ocean and adjacent seas and oceans. *Geological Society of America Bulletin*, 76(7), 803–832.
6. Borges, P., Federiche, A., Train, S., & Rodrigues, L. C. (2008). Spatial and temporal variation of phytoplankton in two subtropical Brazilian reservoirs. *Hydrobiologia*, 607, 63–74.
7. Bravard, J. P., & Peiry, J. L. (1999). The CM pattern as a tool for the classification of alluvial suites and floodplains along the river continuum. *Geological Society, London, Special Publications*, 163(1), 259–268.
8. DGM (1999). *Geology and Mineral Resources Map (1:200 000), Da Lat–Cam Ranh sheet (C-49-I & C-49-II)*. Department of Geology and Minerals of Vietnam.
9. Folk, R. L. (1980). *Petrology of sedimentary rocks*. Hemphill publishing company.
10. Hasle, G. R., Syvertsen, E. E., Steidinger, K. A., Tangen, K., & Tomas, C. R. (1996). *Identifying marine diatoms and dinoflagellates*. Elsevier.
11. Kilham, P., Kilham, S. S., & Hecky, R. E. (1986). Hypothesized resource relationships among African planktonic diatoms. *Limnology and Oceanography*, 31, 1169–1181.
12. Krammer, K., & Lange-Bertalot, H. (1986–1991). *Bacillariophyceae. Teil 1–4* in H. Ettl, J. Gerloff, H. Heynig, and D. Mollenhauer (editors). *Süßwasserflora von Mitteleuropa*. Gustav Fischer Verlag.
13. Moore, D. M., & Reynolds, R. J. (1989). *X-ray Diffraction and the Identification and Analysis of Clay Minerals*. Cambridge University Press.
14. Naito, K., Suzuki, M., Mito, S., Hasegawa, H., Matsui, M., & Imai, I. (2006). Effects of the substances secreted from *Closterium aciculare* (Charophyceae, Chlorophyta) on the growth of freshwater phytoplankton under iron-deficient conditions. *Plankton and Benthos Research*, 1(4), 191–199.

15. Ognjanova-Rumenova, N., & Yaneva, M. (2018). Palaeoecological analysis and environmental development of the Kostenets Neogene Basin, Bulgaria.
16. Phong, M. T., & Dang, T. D. M. (2012). Preparation of filter aids based on Lam Dong diatomite. *Vietnam Journal of Science and Technology*, 50(1), 63–71.
17. Reynolds, C. S., Huszar, V., Kruk, C., Naselli-Flores, L., & Melo, S. (2002). Towards a functional classification of the freshwater phytoplankton. *J. Plankton Res.* 24, 417–428.
18. Round, F. E. (1990). *The Diatoms: Biology and Morphology of the Genera* (Vol. 747). Cambridge University Press.
19. Suhry, H. C., Soeprbowati, T. R., & Jumari, J. (2020). Water quality and pollution index in Galela lake (Kualitas air dan Indeks Pencemaran Danau Galela). *J Ilmu Lingkungan*, 18(2), 236–241. <https://doi.org/10.14710/jil.18.2.236-241>.
20. Tsai, W. T., Lai, C. W., & Hsien, K. J. (2006). Characterization and adsorption properties of diatomaceous earth modified by hydrofluoric acid etching. *Journal of Colloid and Interface Science*, 297(2), 749–754.
21. Vyverman, W. (1996). The Indo-Malaysian North-Australian phycogeographical region revised. *Hydrobiologia*, 336, 107–120.
22. Yang, X., Anderson, N. J., Dong, X., & Shen, J. (2008). Surface sediment diatom assemblages and epilimnetic total phosphorus in large, shallow lakes of the Yangtze floodplain: their relationships and implications for assessing long-term eutrophication. *Freshwater Biology*, 53, 1273–1290. [https://doi.org/10.1002/1099-1085\(200011/12\)14:16/17](https://doi.org/10.1002/1099-1085(200011/12)14:16/17).